This is the accepted manuscript made available via CHORUS. The article has been published as:

Depolarization of nearly spherical particles: The Debye series approach

Lei Bi, Feng Xu, and Gérard Gouesbet

Phys. Rev. A **98**, 053809 — Published 7 November 2018

DOI: 10.1103/PhysRevA.98.053809

Depolarization of nearly spherical particles: the Debye series approach

Lei Bi,[1,*] Feng Xu,[2] and Gérard Gouesbet[3]

*bilei@zju.edu.cn

[1]*Department of Atmospheric Sciences, Zhejiang University, China*
[2]*Jet Propulsion Laboratory, California Institute of Technology, Pasadena, California 91109, USA*
[3]*UMR 6614/CORIA, CNRS, Université et INSA de Rouen, Site du Madrillet, Avenue de l'Université, BP12 76801 Saint Etienne du Rouvray, France*

Abstract

Backscattering depolarization of non-spherical particles plays a critical role in active LiDAR retrievals of cloud or aerosol parameters, as well as in particle characterization techniques. However, the interpretation of backscattering light from particles is a challenging research subject. This study addresses the depolarization of nearly spherical particles by using the Debye series approach. Specifically, the T-matrix is represented as an infinite sum of terms; the terms in the expansion are correspondingly associated with diffraction and reflection ($p = 0$), and multiple transmissions ($p > 0$) from the particle to medium as waves undergo internal reflections. We found that the enhanced depolarization for optically soft particles stems from multiple transmissions. However, this is mostly from the transmission after one internal reflection ($p = 2$), when the refractive index is larger than 1.3. Moreover, the interference among multiple transmissions was found to play an essential role in suppressing the depolarization ratio as the refractive index approaches unity. These findings have implications in interpreting the backscattering optical properties of atmospheric aerosols and hydrosols in water.

1. Introduction

The polarized LiDAR can obtain fruitful microphysical information about atmospheric aerosols and hydrometeors. As a critical quantity, the linear depolarization ratio (LDR) is most frequently used to discriminate cloud phase or aerosol types [1-3]. Thus, extensive theoretical studies, laboratory measurements, and field campaigns have been carried out to understand the depolarization capabilities of various atmospheric particles [4]. In addition to the application of atmospheric detection and retrievals of cloud or aerosol parameters, the LDR (near-backscattering, in particular) can be also used in particle characterization techniques to obtain the microphysical information of particle systems in laboratory [5]. However, there is no simple relation between the LDRs and the particle shape and refractive index. For example, the LDRs peaking at aspect ratios of spheroids very close to unity was discovered by Mishchenko and Hovenier [6] and illustrates the inherent difficulty of treating the LDR as an indicator of the degree of particle non-sphericity.

Owing to the advances on the invariant imbedding T-matrix method (II-TM) [7-10], recently, depolarization capabilities of non-spherical particles have been extensively assessed in a

super-ellipsoidal space and with a large range of refractive indices [11]. It has been shown that the enhanced LDRs are relatively common for optically soft particles (a range of refractive index from 1.05-1.20). Also, the large LDRs exist for nearly spherical particles in a refractive regime with the real part ranging from 1.3 to 1.7. However, the physical mechanism leading to the enhanced LDRs is unclear. As an example, Figure 1 shows the LDRs of prolate spheroids (top panel) and oblate spheroids (bottom panel) as functions of the size parameter and refractive index. It is evident that the pronounced LDRs locate at two ranges of refractive indices, namely (1.05,1.2) and (1.3,1.6).

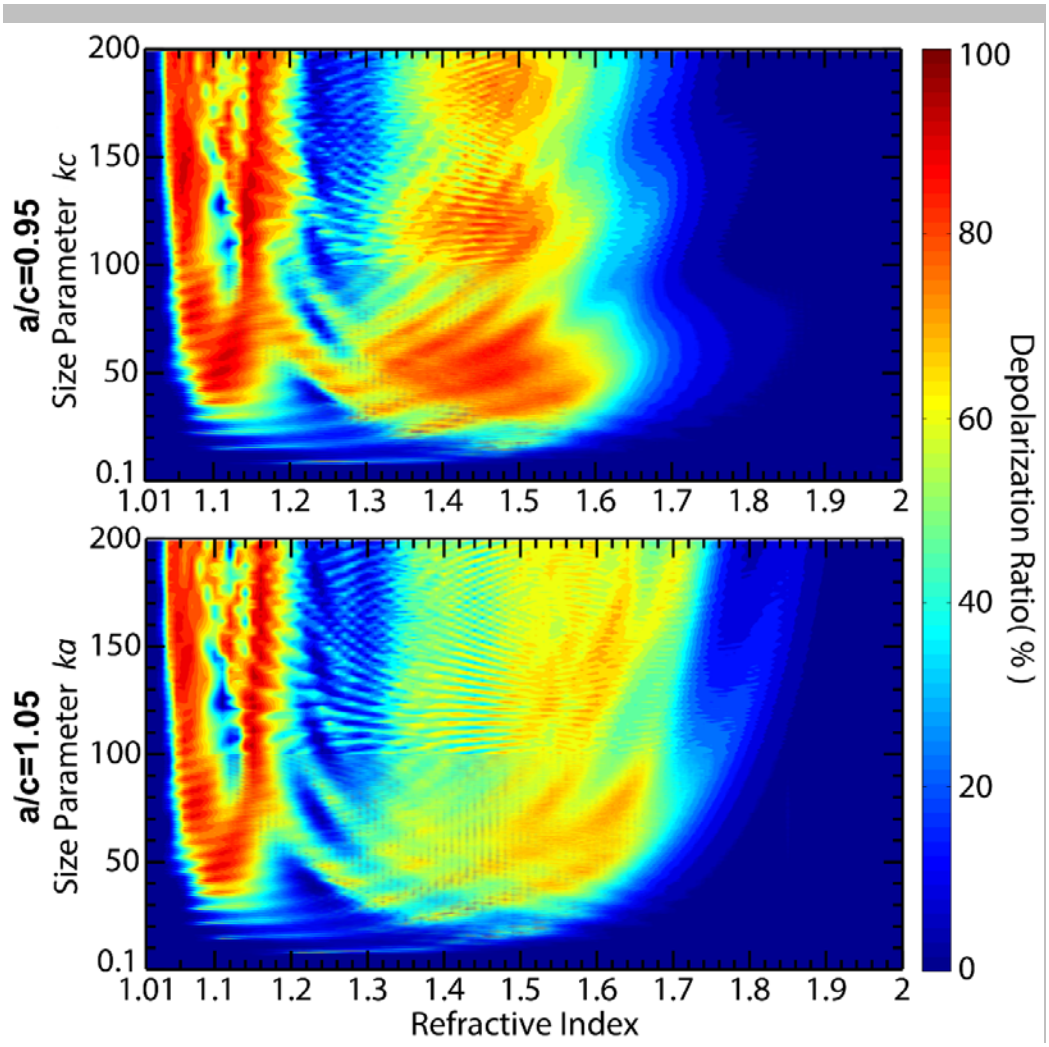

Fig. 1. LDRs for randomly oriented spheroids (aspect ratio is 0.95 and 1.05). The horizontal and vertical axes of a spheroid are denoted as a and c, respectively. $k=2\pi/\lambda$, where λ is the wavelength of the incident light.

It is not straightforward to understand the scattering mechanism leading to the phenomenon above, because the T-matrix solution contains all the effects that contribute to the scattering. This study is indented to provide an in-depth analysis of the depolarization in the framework of Debye's series. The Debye series was first proposed by Debye for an infinite circular cylinder [12], and then has been extensively used for spherical particles [13-16], coated spherical particles [17-23], coated cylinder [24] and further extended to spheroidal particles based on the separation of the variable

method [25-26]. The recent development of Debye's approach for non-spherical particles with the extended boundary condition method (EBCM) [27-28] is a breakthrough that makes it possible to perform accurate analyzes of the scattering mechanism by non-spherical particles. The concept of Debye's series is similar to the geometric optics (GO) approach. In the GO approach, the incident beam consists of a bundle of rays. When a geometric ray is incident upon a particle, it will be partially reflected, and partially refracted into the particle, which could be absorbed into the particle or undergo an arbitrary number of internal reflections. In conjunction with each internal reflection, there will be transmitted rays from the particle to the medium, which contributes to the scattering. Different from the GO, the Debye approach is rooted rigorously in the framework of Maxwell's equations. Each term in the Debye series contains the information of the GO, but also includes semi-classical effects that cannot be interpreted in the GO [29-31]. According to the conventional notations for a sphere, the zeroth-order term (p = 0) corresponds to diffraction and reflection by particle surfaces (note that the diffraction and external reflection are essentially bundled together, but can be separated from each other approximately based on the GO and physical-geometric optics approaches), and the p^{th} term indicates the contribution to scattering from transmitted waves after making p-1 internal reflections.

In this paper, we explore the powerfulness of Debye-series-based T-matrix method, and in particular, interpret the depolarization of incident polarized electromagnetic waves by nearly non-spherical particles, assumed to be spheroids with an aspect ratio close to unity. To analyze depolarization, an explicit formalism is developed in this study by expanding the T-matrix in terms of Debye's series. The EBCM is used to compute reflection and transmission matrices in the Debye's series (See details in Section 2). Thus, the phase matrices associated with each order of Debye's series for either oriented particles or randomly oriented particles could be accurately obtained. Specifically, the contributions from waves associated with diffraction, external reflection, and transmission (with and without interference) can be cleary identified. This paper is organized as follows. In Section 2, we briefly summarize the theoretical formalism that represents the T-matrix as a series. Representative results with discussions are given in Section 3. Section 4 is the summary and conclusion of this study.

2. Theoretical Formalism

Here, we outline a formalism that is developed to assess the underlying mechanism of backscattering. In the framework of the T-matrix, the incident field and the scattered field are expanded in terms of vector spherical wave functions [32]:

$$\mathbf{E}^{inc}(\mathbf{r}) = \sum_{l=1}^{\infty} a_l \mathrm{Rg}\mathbf{M}_l(k\mathbf{r}) + b_l \mathrm{Rg}\mathbf{N}_l(k\mathbf{r}), \tag{1}$$

$$\mathbf{E}^{sca}(\mathbf{r}) = \sum_{l=1}^{\infty} p_l \mathbf{M}_l(k\mathbf{r}) + q_l \mathbf{N}_l(k\mathbf{r}), \tag{2}$$

where k is the wave vector in the medium, $\mathrm{Rg}\mathbf{M}_l$ and $\mathrm{Rg}\mathbf{N}_l$ are the regular vector spherical functions, and $\mathbf{M}_l$ and $\mathbf{N}_l$ are the irregular vector spherical functions. For simplicity, two

subindices of vector spherical functions are combined as one index via $l = n(n+1)+m$, where n is the total angular momentum, and m is the projected angular momentum. The T-matrix $\mathbf{T}$ is defined as a transition matrix that transfers the coefficients of the incident field to those of the scattered field. Explicitly, we have the following equation:

$$\begin{bmatrix} p_1 \\ q_1 \\ \vdots \\ p_{l_{\max}} \\ q_{l_{\max}} \end{bmatrix} = \begin{bmatrix} \mathrm{T}_{11}^{11} & \mathrm{T}_{11}^{12} & \cdots & \mathrm{T}_{1l_{\max}}^{11} & \mathrm{T}_{1l_{\max}}^{12} \\ \mathrm{T}_{11}^{21} & \mathrm{T}_{11}^{22} & \cdots & \mathrm{T}_{1l_{\max}}^{21} & \mathrm{T}_{1l_{\max}}^{22} \\ \vdots & \vdots & \cdots & \vdots & \vdots \\ \mathrm{T}_{l_{\max}1}^{11} & \mathrm{T}_{l_{\max}1}^{12} & \cdots & \mathrm{T}_{l_{\max}l_{\max}}^{11} & \mathrm{T}_{l_{\max}l_{\max}}^{12} \\ \mathrm{T}_{l_{\max}1}^{21} & \mathrm{T}_{l_{\max}1}^{22} & \cdots & \mathrm{T}_{l_{\max}l_{\max}}^{21} & \mathrm{T}_{l_{\max}l_{\max}}^{22} \end{bmatrix} \begin{bmatrix} a_1 \\ b_1 \\ \vdots \\ a_{l_{\max}} \\ b_{l_{\max}} \end{bmatrix}, \tag{3}$$

where $l_{\max}$ is the truncation number. Based on the Debye's concept, the T-matrix can be expanded in terms of a series:

$$\mathbf{T} = -\frac{1}{2}\left[\mathbf{1} - \tilde{\mathbf{R}}_{11} - \tilde{\mathbf{T}}_{21}\left(\sum_{n=0}^{\infty}\left(\tilde{\mathbf{R}}_{22}\right)^n\right)\tilde{\mathbf{T}}_{21}\right] = -\frac{1}{2}\left[\mathbf{1} - \tilde{\mathbf{R}}_{11} - \tilde{\mathbf{T}}_{12}\frac{1}{\mathbf{1}-\tilde{\mathbf{R}}_{22}}\tilde{\mathbf{T}}_{21}\right], \tag{4}$$

where $\tilde{\mathbf{R}}_{11}$ is defined as a matrix that transforms the coefficient of the incident vector spherical wave field to those of the reflected field, $\tilde{\mathbf{T}}_{21}$ is defined as a matrix that transforms the coefficient of the incident vector spherical wave field to those of the refracted field, $\tilde{\mathbf{R}}_{22}$ is defined as a matrix that transforms the coefficient of the internal outgoing vector spherical wave field to those of the reflection field within the particle, and $\tilde{\mathbf{T}}_{12}$ is defined as a matrix that transforms the coefficient of the internal outgoing vector spherical wave field to those of the transmitted field exiting the particle. $\tilde{\mathbf{R}}_{11}$, $\tilde{\mathbf{T}}_{21}$, $\tilde{\mathbf{R}}_{22}$, and $\tilde{\mathbf{T}}_{12}$ are computed from the EBCM [27]. Note that the sub-indices (11,12,21,22) in Eq. (4) are not intended to indicate the elements of matrices but symbolize the particle (as 2) and the medium (as 1). The first equality of Eq. (4) is obtained from physical concept involved in Debye's series. It can be directly validated for homogeneous spherical particles, which have analytical solutions. However, for non-spherical particles, it is not straightforward to prove Eq. (4), because analytical solutions do not exist. Instead, Eq. (4) has been numerically validated through the second equality to avoid truncation errors in summation; the left and right sides are computed from the II-TM and the EBCM, respectively. The agreement of phase matrices computed from the both sides of Eq. (4) also indirectly verified the equation (shown in Section 3).

To separate the contributions from diffraction, reflection, and higher order transmissions, the following quantities are defined:

$$\mathbf{T}_0 = -\frac{1}{2}\left[\mathbf{1} - \tilde{\mathbf{R}}_{11}\right], \tag{5}$$

$$\mathbf{T}_1 = \frac{1}{2}\tilde{\mathbf{T}}_{12}\tilde{\mathbf{T}}_{21}, \tag{6}$$

$$\mathbf{T}_2 = \frac{1}{2}\tilde{\mathbf{T}}_{12}\tilde{\mathbf{R}}_{22}\tilde{\mathbf{T}}_{21}, \tag{7}$$

$$\mathbf{T}_N = \frac{1}{2}\tilde{\mathbf{T}}_{12}\left(\tilde{\mathbf{R}}_{22}\right)^{N-1}\tilde{\mathbf{T}}_{21}, N \geq 1, \tag{8}$$

$$\mathbf{T}_{\mathrm{p<=N}} = \sum_{k=0}^{N}\mathbf{T}_k = -\frac{1}{2}\left[\mathbf{1} - \tilde{\mathbf{R}}_{11} - \tilde{\mathbf{T}}_{12}\left(\sum_{n=0}^{N-1}\left(\tilde{\mathbf{R}}_{22}\right)^n\right)\tilde{\mathbf{T}}_{21}\right], \tag{9}$$

The physical implications of all the above terms are clear. $\mathbf{T}_0$ contains all the information associated with diffraction and reflection. In particular, the edge effect associated with a tunneling process can be rigorously obtained, which have been studied in Bi et al. [33] and Lin et al. [34]. $\mathbf{T}_1$ contains all the information associated with the contribution to the scattered field from the waves that transmitted to the particle without internal reflection. $\mathbf{T}_N$ represents the contribution from transmitted waves after N-1 internal reflections. For simplicity, $\mathbf{T}_{\mathrm{p<=N}}$ is defined to sum all the contributions up to the N^{th} order. For a polarized plane-wave incident field, the phase matrix can be derived from the T-matrix. The phase matrix of randomly oriented particles (with mirror symmetry) that determines the change in the Stokes vector $\left[I_{inc}, Q_{inc}, U_{inc}, V_{inc}\right]^T$ of the incident wave to that of scattered waves $\left[I_{sca}, Q_{sca}, U_{sca}, V_{sca}\right]^T$ is given by [35]:

$$\begin{bmatrix} I_{sca}(\theta) \\ Q_{sca}(\theta) \\ U_{sca}(\theta) \\ V_{sca}(\theta) \end{bmatrix} \propto \begin{bmatrix} P_{11}(\theta) & P_{12}(\theta) & 0 & 0 \\ P_{21}(\theta) & P_{22}(\theta) & 0 & 0 \\ 0 & 0 & P_{33}(\theta) & P_{34}(\theta) \\ 0 & 0 & P_{43}(\theta) & P_{44}(\theta) \end{bmatrix} \begin{bmatrix} I_{inc} \\ Q_{inc} \\ U_{inc} \\ V_{inc} \end{bmatrix}, \tag{10}$$

where θ is the scattering angle ranging from 0 to 180 degrees, $P_{12}=P_{21}$, and $P_{43}=-P_{34}$. For a linearly polarized incident wave with the Stokes vector $\left[1\ 1\ 0\ 0\right]^T$, the Stokes vector of the scattered wave is $\left[P_{11}+P_{12}\ \ P_{21}+P_{22}\ \ 0\ 0\right]^T$. Given the phase matrix, the LDR (defined as the intensity of electric field perpendicular to the scattering plane $\left|E_{\perp}\right|^2$ to that parallel to the scattering plane $\left|E_{\parallel}\right|^2$) can be straightforwardly computed by:

$$\mathrm{LDR} = \frac{\left|E_{\perp}\right|^2}{\left|E_{\parallel}\right|^2} = \frac{I_{sca} - Q_{sca}}{I_{sca} + Q_{sca}} = \frac{P_{11} - P_{22}}{P_{11} + 2P_{12} + P_{22}} = \frac{1 - P_{22}/P_{11}}{1 + 2P_{12}/P_{11} + P_{22}/P_{11}}. \quad (11)$$

At direct backscattering, the LDR can be shown to be less than or equal to 100%; this is because P_{12} is zero, and $P_{22}/P_{11} \geq 0$ according to the reciprocity theorem [6]. However, for the side scattering, the LDR could be much larger than 100% (To the best of our knowledge, this feature has not been discussed in previous literature; examples will be shown in Section 3).

The concept and technical details of the T-matrix formulation, the II-TM and the EBCM are not iterated here because they were thoroughly described in previous studies [7-10,27,32, 36,37]. The present study focuses on the optical properties of spheroids with aspect ratios close to unity, although other nearly spherical particles could also have enhanced backscattering depolarization.

Now we consider two computational schemes:

(1) Compute the phase matrix from $\mathbf{T}_{p<=N}$, and understand the convergence of T-matrix and contributions of each order waves to the scattered field. Note that the interferences between the different order of waves are taken into account.

(2) Compute the phase matrix from $\mathbf{T}_N$, and then sum all the phase matrices with weighting functions. The comparison of this phase matrix from the summations and the phase matrix computed from the T-matrix can be used to assess the interference effect among the different order of waves. To compute the final phase matrix, the weights, namely, the "scattering cross section" for each term should be computed. The scattering cross sections can be employed to understand the relative contribution of each order of scattered waves. The p-th order scattering cross-section of a randomly oriented particle can be computed from the following formula:

$$C^p{}_{sca} = -\frac{2\pi}{k^2}\sum_{l=1}^{l_{\max}}\sum_{l'=1}^{l_{\max}}\left[\left|\mathrm{T}^{11}_{p,ll'}\right|^2 + \left|\mathrm{T}^{12}_{p,ll'}\right|^2 + \left|\mathrm{T}^{21}_{p,ll'}\right|^2 + \left|\mathrm{T}^{22}_{p,ll'}\right|^2\right]. \quad (12)$$

where $\mathrm{T}^{11}_{p,ll'}$, $\mathrm{T}^{12}_{p,ll'}$, $\mathrm{T}^{21}_{p,ll'}$ and $\mathrm{T}^{22}_{p,ll'}$ are the elements of $\mathbf{T}_p$ (see Eq. (3) for the explicit definition of $\mathbf{T}$). The phase matrix elements neglecting the interference are computed by

$$P_{ij} = \sum_{p=0}^{\infty} P^p{}_{ij} C^p{}_{sca} \quad \mathrm{i,j=1,4} \quad . \quad (13)$$

where $P^p{}_{ij}$ is the phase matrix element computed from the p^{th} order Debye series.

3. Results

3.1 Numerical Validation

Figure 2 shows a comparison of the phase matrix computed from the II-TM and Debye's series. The II-TM directly computes the T-matrix by employing an invariant embedding procedure, whereas the Debye's series approach first computes the reflection and transmission matrices $\tilde{\mathbf{R}}_{11}$,

$\tilde{\mathbf{R}}_{22}$, $\tilde{\mathbf{T}}_{21}$, and $\tilde{\mathbf{T}}_{22}$, and then computes the T-matrix through Eq. (4). Once the T-matrix is obtained, the two methods share the same algorithm to compute the phase matrix of randomly oriented particles. An excellent agreement between the two scattering phase matrixes validates Debye's approach, as well as its numerical implementation. Note that the second formula with the inverse of $\mathbf{1}-\tilde{\mathbf{R}}_{22}$ in Eq. (4) is employed in the computation to avoid possible truncation errors in Figure 2.

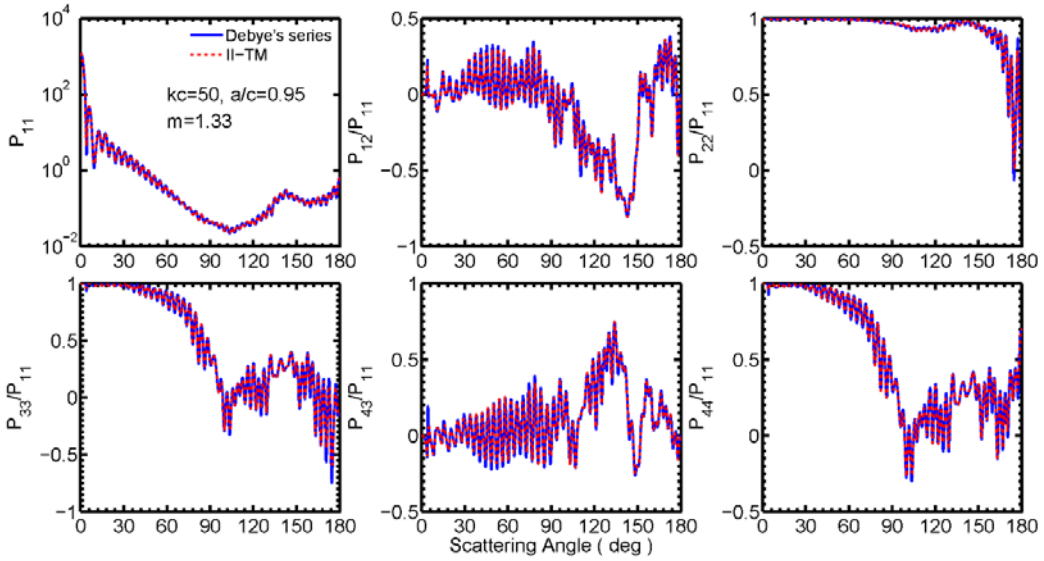

Fig. 2. Comparison of the phase matrix of randomly oriented spheroids (the aspect ratio a/c = 0.95) computed from the invariant imbedding T-matrix and Debye's series. The refractive index is 1.33, and the size parameter is kc = 50.

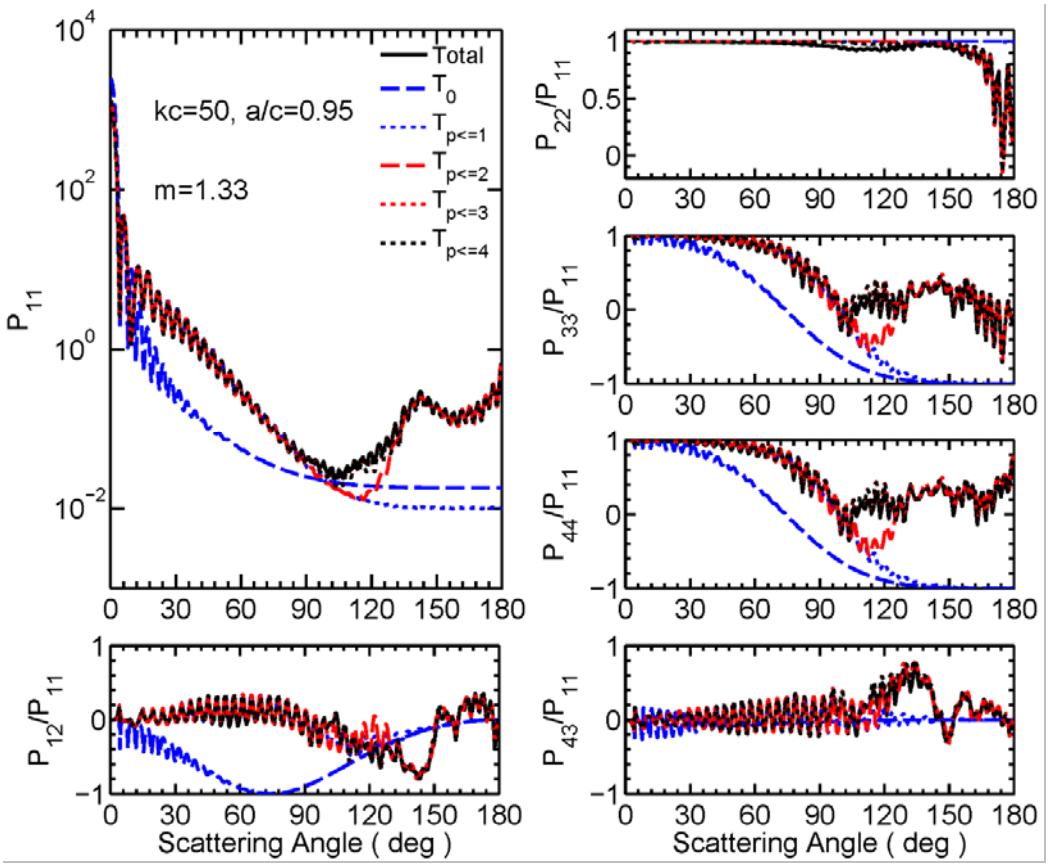

Fig. 3. The contributions of Debye's series of various order to six nonzero phase matrix elements for randomly oriented spheroids with the aspect ratio of 0.95.

Now we turn to the contributions of waves (of various orders) to the phase matrix of randomly oriented spheroids. As expected, the contribution from the diffraction and external reflection to the phase function is featureless, except for a strong diffraction peak. A comparison of the diffraction plus reflections computed from the zeroth-order Debye series and physical optics approximation has been given in Bi and Yang [38], showing an excellent agreement. From this study, it is evident from Figure 3 that the superposition of the first order transmission and diffraction and reflection yields close results with the II-TM for scattering angles less than 85 degrees. Addition of the transmission after one internal refection dominates the scattering contributions in the scattering angle from 130 to 180 degrees. The transmission after two internal reflections has critical contributions to the phase function at scattering angles between 85 and 130. It is evident from Figure 3 that the summation of wave contributions with $p \leq 3$ reasonably explain the phase function computed from the II-TM, although the accuracy can be improved by including higher order terms. However, from the P_{22}/P_{11} comparison, the maximum of summation terms should be sufficiently large (upto a few tens) to guarantee the convergence of P_{22}/P_{11} between 60 and 120 degrees.

3.2 Linear Depolarization Ratios

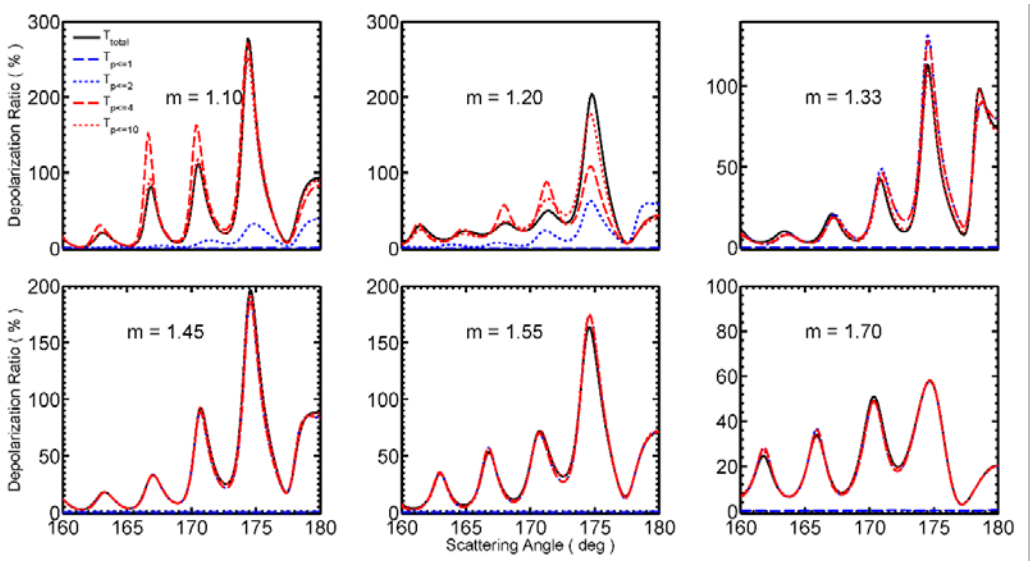

Fig. 4. Depolarization ratios at scattering angles ranging from 160 and 180 degrees for six selected refractive indices. The size parameter is kc = 50. The aspect ratio a/c = 0.95.

For nearly spherical particles, the LDRs are quite small when the scattering angles are less than 160 degrees. Figure 4 shows the depolarization ratio at the scattering angles larger than 160 degrees at six refractive indices. $T_{p<=1}$ indicates the result with transmission without internal reflections. It is evident that the LDR is zero for all the refractive indices. This is because the diffraction and reflection produce no depolarization, and the first order transmission has no contribution to the backscattering scattering angles. For the refractive indices (1.10 and 1.20), a superposition of different orders has an obvious contribution to the depolarization. However, for the refractive indices (1.33, 1.45, 1.55, and 1.70), the contribution from the second order transmission dominate in the backscattering depolarization. A little impact from $p > 2$ can also be seen at the refractive index of 1.33.

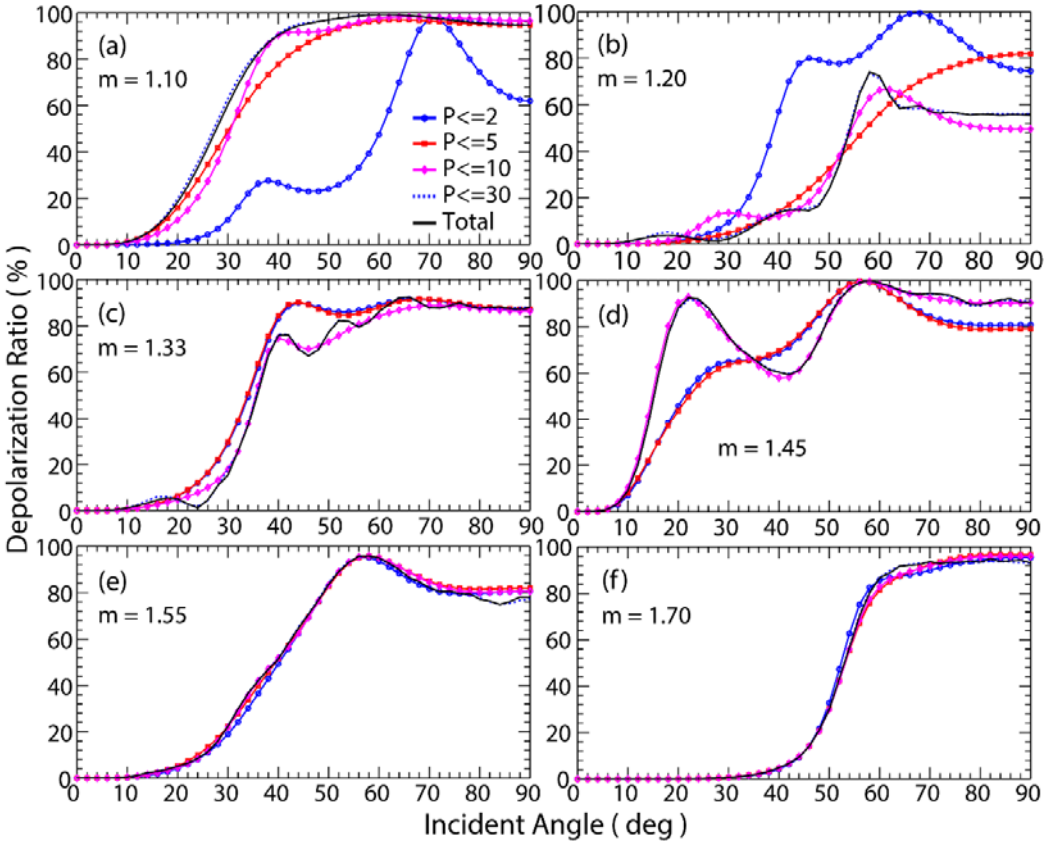

Fig. 5. Depolarization ratios of a particle with different orientations.

Figure 5 shows the comparison of LDR as a function of particle orientation. The incident angle is defined as the angle between the direction of the incident light and the symmetric axis of spheroids. For the refractive index 1.10, high order transmissions could significantly increase the depolarization. However, at the orientation 70^{o}, the depolarization is almost solely from the p = 2 term. At the refractive index 1.20, the multiple transmission decreases the depolarization in general. From Figures 5c–e, we can see that the impact of multiple transmissions becomes smaller and smaller as the refractive index increases.

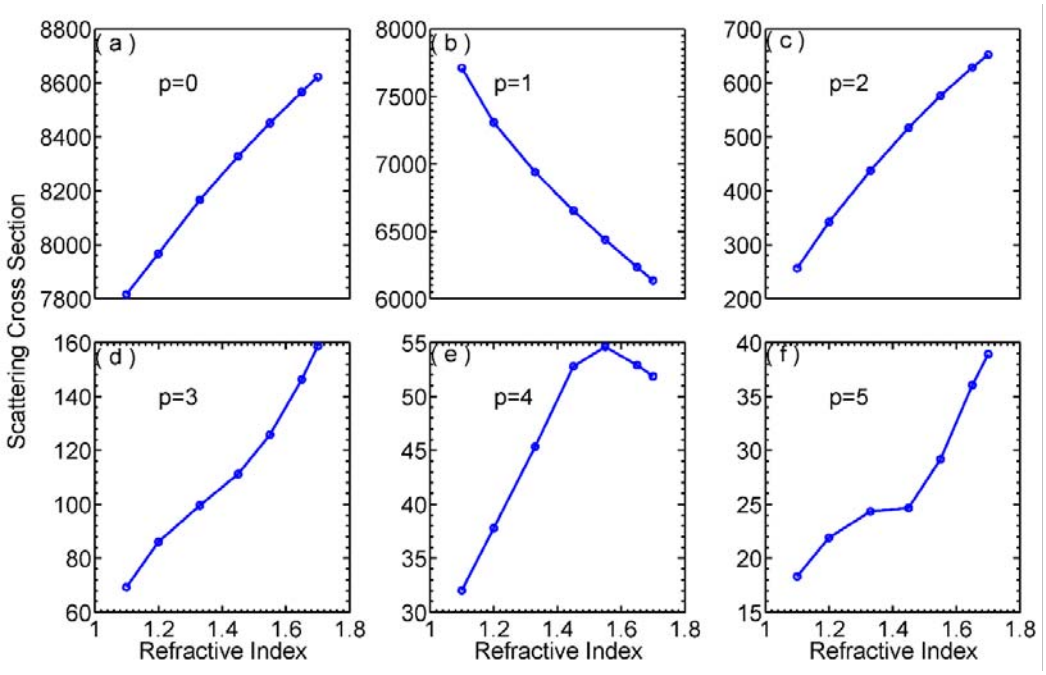

Fig. 6. Scattering cross sections for the different order of waves.

Figure 6 shows the "scattering cross section" as a function of the refractive index. From Figure 6a, we can see that the scattering cross section increases as the refractive index increases. In this case, the diffraction energy is about the averaged projected area, but the energy from reflected light increases as the refractive index increases, whereas the "scattering cross section" associated with the transmission (p = 1) shown in Figure 6b decreases as the refractive index increases. For higher order terms, the scattering cross section could first increase and then decrease as the refractive index increases (see Figure 6e).

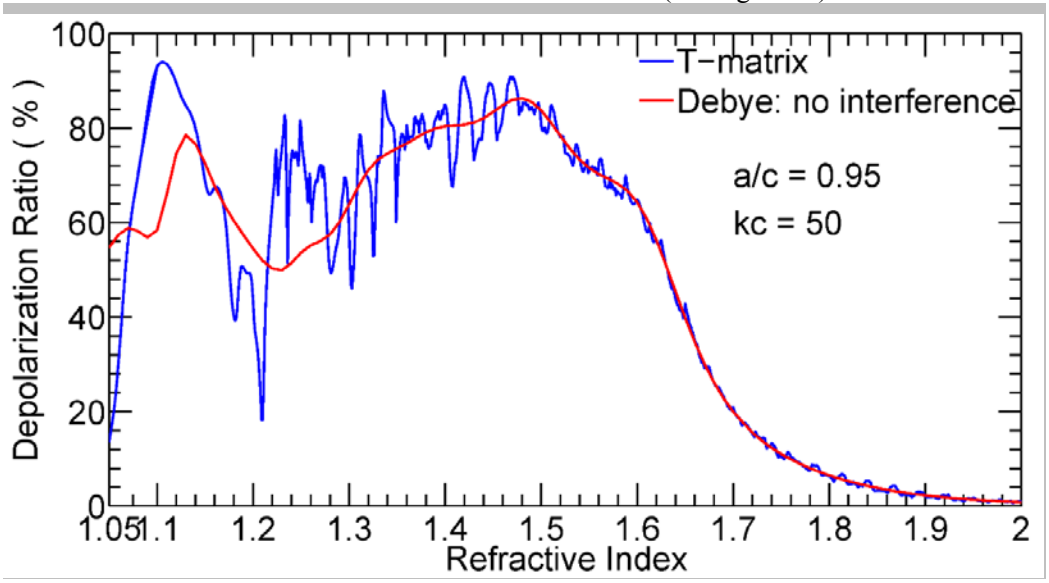

Fig. 7. Interference effect on depolarization ratio.

Based on the scattering cross sections given in Figure 6, the phase matrices neglecting the phase interference can be computed. Thus, the interference effect on the LDR can be investigated. Figure 7 shows the depolarization ratio as a function of the refractive index for randomly oriented spheroids. The blue curve (with high oscillations) is the rigorous solution

computed from the T-matrix method. The red curve (relatively smooth) is computed from the Debye series. However, the interference among the different order of transmissions is neglected. As evident is that the interference can be reasonably neglected for the refractive index larger than 1.5. The main reason for this is that the p = 2 term dominates in the backward scattering. In the 1.3 to 1.5 refractive region, the interference effect is obvious, but the results without interference can still capture the general trend of LDRs as a function of the refractive index. However, as the refractive index decreases, the difference between the two results can be huge. In particular, for the refractive index approaching 1.0, the interference effect plays an essential role in suppressing the depolarization. From this comparison, it is easy to understand how, when ignoring interference, the accuracy of the geometric-optics method becomes poor as the refractive index decreases. Because the LDRs are sensitive to the interference among the different order of waves, modeling LDRs for optically soft particles should be done carefully when modeling the particle geometry and choosing computational methods (geometric optics could lead to large uncertainties).

4. Summary and conclusions

In this paper, we explored the use of Debye's series to compute the phase matrix of spheroids with either random or fixed orientations. By defining the T-matrix with different orders and computing the associated phase matrix, we analyzed the contribution from the different transmitted waves to the scattering. As expected, diffraction and external reflection cause no depolarization. For optically soft particles, the superposition of some transmitted waves is critical to the depolarization. But for a particle with the refractive index larger than 1.3, the depolarization of backscattered light is dominated by the p = 2 terms. Namely, the backscattering contributed to the transmission after one internal reflection. These findings have strong implications in LiDAR retrievals of cloud or aerosol parameters, as well as in particle characterization techniques. At present, this study only focuses on nearly spherical particles. The existing formalism of T-matrix Debye series [27] is applicable to other convex-shape non-spherical particles than spheroids discussed here. However, some efforts on numerical implementation are necessary to decompose the electromagnetic scattering by large-size and large-aspect ratio particles (such as particles with size parameter over 100 and aspect ratio over 3-5). One highly possible way to resolve this constraint is to apply the invariant imbedding procedure [7] to Debye series, which has been proved by our progress on calculating total light scattering by arbitrarily shaped large non-spherical particles [8-10]. These will be our future research subject.

Acknowledgments

Dr. Lei Bi was supported by the National Natural Science Foundation of China (41675025), and the Fundamental Research Funds for the Central Universities (2017QNA3017). The work by co-author Feng Xu was carried out at the Jet Propulsion Laboratory, California Institute of Technology under a contract with the National Aeronautics and Space Administration.

References:

1. D. M. Winker, M. A. Vaughan, A. Omar, Y. Hu, K. A. Powell, Z. Liu, W. H. Hunt, and S. A. Young, "Overview of the CALIPSO mission and CALIOP data processing algorithms," J. Atmos. Ocean. Technol. 26(11), 2310–2323 (2009).
2. Y. Hu, M. Vaughan, Z. Liu, B. Lin, P. Yang, D. Flittner, B. Hunt, R. Kuehn, J. Huang, D. Wu, S. Rodier, K. Powell, C. Trepte, and D. Winker, "The depolarization-attenuated backscatter relation: CALIPSO lidar measurements vs. theory," Opt. Express 15(9), 5327–5332 (2007).
3. L. Bi, W. Lin, Z. Wang, X. Tang, X. Zhang, and B. Yi, "Optical modeling of sea salt aerosols: the effects of nonsphericity and inhomogeneity," Journal of Geophysical Research Atmospheres, 123, 543–558 (2018). https://doi.org/10.1002/2017JD027869
4. K. Sassen, "The polarization lidar technique for cloud research: a review and current assessment," Bull. Am. Meteorol. Soc. 72(12), 1848–1866 (1991).

5. E. Järvinen, O. Kemppinen, T. Nousiainen, T. Kociok, O. Möhler, T. Leisner and M. Schnaiter, “Laboratory investigations of mineral dust near-backscattering depolarization ratios,” J. Quant. Spectrosc. Radiat. Transf. 178, 192–208 (2016).
6. M. I. Mishchenko and J. W. Hovenier, “Depolarization of light backscattered by randomly oriented nonspherical particles,” Opt. Lett. 20(12), 1356–1358 (1995).
7. B. R. Johnson, “Invariant imbedding T-matrix approach to electromagnetic scattering,” App. Opt. 27, 4861–4873 (1988).
8. L. Bi, P. Yang, G. W. Kattawar, and M. I. Mishchenko, “Efficient implementation of the invariant imbedding T-matrix method and the separation of variables method applied to large nonspherical inhomogeneous particles,” J. Quant. Spectrosc. Radiat. Transfer, 116, 169–183 (2013).
9. L. Bi, P. Yang, G. W. Kattawar, and M. I. Mishchenko, “A numerical combination of extended boundary condition method and invariant imbedding method to light scattering by large spheroids and cylinders,” J. Quant. Spectrosc. Radiat. Transfer, 123, 17–22 (2013).
10. L. Bi and P. Yang, “Accurate simulation of the optical properties of atmospheric ice crystals with invariant imbedding T-matrix method,” J. Quant. Spectrosc. Radiat. Transfer. 138, 17–35 (2014).
11. L. Bi, W. Lin, D. Liu, and K. Zhang, “Assessing the depolarization capabilities of nonspherical particles in a super-ellipsoidal shape space,” Optics Express, 26(2) 1726–1742 (2018).
12. P. Debye, Phys. Zeit. 9, 775 (1908). SPIE Milestone Series Vol. MS89 (1994), pp. 198-204 (in English)].
13. B. Van der Pol and H. Bremmer, Philos. Mag. 24, 141, 823 (1937).
14. J. A. Lock, “Cooperative effects among partial waves in Mie scattering,” J. Opt. Soc. Am. A 5, 2032–2044 (1988).
15. G. Gouesbet, “Debye Series Formulation for Generalized Lorenz - Mie Theory with the Bromwich Method,” Part. Part. Syst. Charact. 20, 382–386,(2003).
16. J. A. Lock, “Semiclassical scattering of an electric dipole source inside a spherical particle,” J. Opt. Soc. Am. A 18, 3085–3097 (2001).
17. J. A. Lock, J. M. Jamison, and C.-Y. Lin, “Rainbow scattering by a coated sphere,” Appl. Opt. 33, 4677 (1994).
18. J. A. Lock, “Debye series analysis of scattering of a plane wave by a spherical Bragg grating,” Appl. Opt. 44, 5594–5603 (2005).
19. J. A. Lock, “Scattering of an electromagnetic plane wave by a Luneburg lens. II. Wave theory,” J. Opt. Soc. Am. A 25, 2980–2990 (2008).
20. R. Li, X. Han, L. Shi, K. F. Ren, and H. Jiang, “Debye series for Gaussian beam scattering by a multilayered sphere,” Appl. Opt. 46, 4804–4812 (2007).
21. J. A. Lock, “Linear system approach to the Debye series for electromagnetic scattering by a multi-layer sphere: A tutorial,” J. Quant. Spectrosc. Radiat. Transfer 178, 38–49 (2016)
22. J. A. Lock and P. Laven, "Understanding light scattering by a coated sphere Part 1: Theoretical considerations," J. Opt. Soc. Am. A 29, 1489–1497 (2012)
23. P. Laven and J. A. Lock, "Understanding light scattering by a coated sphere Part 2: Time domain analysis," J. Opt. Soc. Am. A 29, 1498-1507 (2012)
24. Z. Wu and H. Li, “Debye series of scattering by a multi-layered cylinder in an off-Axis 2D Gaussian beam,” Chin. Phys. Lett. 25, 1672 (2008).
25. J. A. Lock, and F. Xu, "Optical caustics observed in light scattered by an oblate spheroid," Appl. Opt. 49, 1288–1304 (2010)
26. F. Xu, J. A. Lock, and C. Tropea, “Debye series for light scattering by a spheroid,” J. Opt. Soc. Am. A 27, 671 (2010).
27. F. Xu, J. A. Lock, and G. Gouesbet, “Debye series for light scattering by a nonspherical particle,” Phys. Rev. A 81, 043824 (2010).
28. F. Xu, and J. A. Lock, “Debye series for light scattering by a coated non-spherical particle,” Phys Rev A 81, 063812 (2010)
29. E. A. Hovenac and J. A. Lock, “Assessing the contribution of surface waves and complex rays to far-field Mie scattering by use of the Debye series,” J. Opt. Soc. Am. A 9, 781 (1992).
30. H. M. Nussenzveig and W. J. Wiscombe, “Efficiency factors in Mie scattering,”Phys. Rev. Lett. 59, 1667 (1987).

31. L. Bi, P. Yang, G. W. Kattawar, and R. Kahn, **"**Single-scattering properties of tri-axial ellipsoidal particles for a size parameter range from Rayleigh to geometric-optics regimes," Appl. Opt. 48, 114–126 (2009).
32. M. I. Mishchenko, L. D. Travis, A. A. Lacis Scattering, absorption and emission of light by small particles. Cambridge: Cambridge University Press; 2002.
33. L. Bi, P. Yang, G. W. Kattawar, and M. I. Mishchenko, "Optical tunneling of arbitrary macroscopic 3D objects," Phys. Rev. A. 92,013814 (2015).
34. W. Lin, L. Bi, D. Liu, and K. Zhang, "Use of Debye's series to determine the optimal edge-effect terms for computing the extinction efficiencies of spheroids," Optics Express, 25(17), 20298-20312 (2017).
35. H. C. van de Hulst, Light Scattering by Small Particles (Dover, 1981).
36.] G. Gouesbet, "T-matrix formulation and generalized Lorenz-Mie theories in spherical coordinates, " Optics Communications, 283:517–521 (2010).
37. G. Gouesbet and J.A. Lock, "On the electromagnetic scattering of arbitrary shaped beams by arbitrary shaped particles: A review," Journal of Quantitative Spectroscopy and Radiative Transfer, 162, 31–49 (2015).
38. L. Bi, and P. Yang, "Tunneling effects in electromagnetic wave scattering by nonspherical particles: A comparison of the Debye series and physical-geometric optics approximations," J. Quant. Spectrosc. Radiat. Transfer, 178,93–107 (2015).